(2)

DEPARTMENT OF PHYSICS
OLD DOMINION UNIVERSITY
COLLEGE OF SCIENCES
NORFOLK, VIRGINIA 23529

Technical Report No. PTR 90-4

SDIO/IST ULTRASHORT WAVELENGTH LASER

"Novel Experimental Schemes for Observing the Mössbauer Effect in Long-Lived Nuclear Levels and Nuclear Coherent States"

By

Gilbert R. Hoy, Principal Investigator

Final Report
For the period ended May 26, 1990

Prepared for
Naval Research Laboratory
4555 Overlook Avenue, S.W.
Washington, D.C. 20375-5000

Under
Research Contract N00014-87-K-2015
Dr. P. Kepple, Scientific Officer

May 1990

Old Dominion University Research Foundation is a not-for-profit corporation closely affiliated with Old Dominion University and serves as the University's fiscal and administrative agent for sponsored programs.

Any questions or comments concerning the material contained in this report should be addressed to:

Executive Director
Old Dominion University Research Foundation
P. O. Box 6369
Norfolk, Virginia 23508-0369

Telephone: (804) 683-4293
Fax Number: (804) 683-5290

DEPARTMENT OF PHYSICS
OLD DOMINION UNIVERSITY
COLLEGE OF SCIENCES
NORFOLK, VIRGINIA 23529

Technical Report No. PTR 90-4

SDIO/IST ULTRASHORT WAVELENGTH LASER

"Novel Experimental Schemes for Observing the Mössbauer Effect in Long-Lived Nuclear Levels and Nuclear Coherent States"

By

Gilbert R. Hoy, Principal Investigator

Final Report
For the period ended May 26, 1990

Prepared for
Naval Research Laboratory
4555 Overlook Avenue, S.W.
Washington, D.C. 20375-5000

Under
Research Contract N00014-87-K-2015
Dr. P. Kepple, Scientific Officer

Submitted by the
Old Dominion University Research Foundation
P.O. Box 6369
Norfolk, Virginia 23508-0369

May 1990

SDIO/IST ULTRASHORT WAVELENGTH LASER

FINAL REPORT

"Novel Experimental Schemes for Observing the Mössbauer Effect in Long-Lived Nuclear Levels and Nuclear Coherent States"

by
Gilbert R. Hoy

I. OUTLINE OF THIS FINAL REPORT

This report is organized in the following way. Section II contains some general remarks concerning: our overall research effort, the students involved in this project, as well as scientific collaborations. In Section III a summary of the results contained in our previous reports is given. Section IV contains a rather complete description of our research efforts involving the search for the Mössbauer effect (M.E.) in ^{109}Ag. Some results contained in previous reports are included for completeness. This section includes a theoretical formulation of the problem as well as the experimental procedures used. A theoretical extension of our earlier parametric formulation allows us to make model calculations that approximate physical reality. We also discuss a new experimental technique for detecting recoilless γ-ray transitions in long-lived nuclear levels. In Section V our conclusions are presented.

II. GENERAL REMARKS

Our research has dealt primarily with the search for the M.E. in ^{109}Ag from both the experimental and theoretical points of view[1-4]. The experiments were carried out in both the vertical and horizontal geometries. Mr. Shokrollah Rezaie-Serej, the senior graduate student working on this project, will complete his Ph.D. dissertation on this subject within the next year. Two students, Hsing-Ching Chang and Jialin Zeng, have left our group after determining that experimental physics was not what they really wanted to do. However, two new students, Walter (Mike) C. McDermott and David Johnson, have recently joined our group.

Dr. R. Dean Taylor (Los Alamos National Laboratory) has collaborated with us, particularly, by providing the radioactively doped samples used in our ^{109}Ag studies. Isotope Products Laboratories is currently preparing radioactive samples to be used in our continuing efforts to observe multibeam Borrmann modes using γ rays.

III. SUMMARY OF PREVIOUS REPORTS

In our previous reports we have described our initial experimental and theoretical procedures used in the search for the M.E. effect in ^{109}Ag. Our preliminary results for detecting the M.E. in ^{109}Ag using the vertical geometry has also been presented. Furthermore, we have shown that the application of a time dependent applied magnetic field may prove useful in determining the extent of the M.E. , as well as giving an estimation of the size of inhomogeneous fields in single crystals.

We also have presented calculations dealing with the propagation of multibeam Borrmann radiation modes. These have included calculations for face centered cubic and body centered cubic crystals. The resulting mode cone angles have been calculated for a number of cases. The propagation properties of a six-beam radiation mode has been calculated in detail although there does appear to be a mistake in the calculation which has yet to be corrected. However, the calculations of the eigenmodes of the radiation field seem to be correct. It is the propagation properties of these eigenmodes that contain an error. Pictorial representations of the symmetry of reciprocal lattice planes, basis polarization vectors, and eigenvectors for the six-beam radiation mode have been given.

IV. SEARCH FOR THE MÖSSBAUER EFFECT IN ^{109}Ag

Since nuclear-resonant γ-ray transitions having narrow linewidths are a prerequisite for the operation of γ-ray lasers, it is of interest to know how narrow the linewidth of a recoillessly emitted or absorbed γ ray can actually be. There is a practical limit set by inhomogeneities that exist in real single crystals. The first-excited nuclear level of ^{109}Ag has a half-life of about 40 sec and a corresponding natural linewidth of approximately 10^{-17} eV. This is obviously a difficult case for the observation of the M.E. considering the size of the quoted[5] lower limit for inhomogeneous line-broadening effects in real crystals of 10^{-13} eV. Therefore, a successful observation of the M.E. in ^{109}Ag will provide valuable information on the practical limit of ultra-narrow lines and the size of the related line-broadening mechanisms in real crystals.

As noted above, we have been engaged in a detailed study searching for the M.E. in ^{109}Ag using silver single crystals. Other researchers[6-8] have produced evidence for such an effect but detailed corroborating results are needed. Wildner and Gonser[8] used the temperature dependence of the self-absorption of γ rays in a ^{109}Cd-doped silver single crystal to detect the

occurrence of the M.E.. Following their pioneering method, we have, in addition, monitored the self-absorption of the ^{109}Cd x rays to account for counting-rate changes at different temperatures due to solid-angle effects. Furthermore, in our method we obtain the ratio of x-ray to γ-ray counts as a function of temperature, and thus attempt to observe the relative increase in this ratio at low temperatures corresponding to the decrease in the γ-ray counts due to the M.E.. The primary advantages of using the ratio are that the time dependence due to the source decay, and the solid angle effects, to first order, cancel out.

A. Formulation of the problem: parametric approach

In analyzing our data, we have considered several factors: the distribution of radioactive nuclei in the sample, the contraction of the sample, sample mount, and internal components of our helium crystat as the temperature is lowered, and the solid angle contributions from different layers of the sample. We assume that the distribution of the source nuclei, ^{109}Cd, in the silver sample follows the usual Gaussian distribution[9] as shown in Eq. (1). The value of α depends on the diffusion constant for ^{109}Cd in silver, and the temperature and time of the anneal.

$$C(x) = C_0 e^{-\alpha x^2} \qquad (1)$$

where C_0 is the source density per unit length.

If the radius of the cylindrical detector is a and the radius of the cylindrical sample is b in a coaxial configuration, the geometrical solid-angle factor for a particular sample slice located by x in Fig. 1 ,corresponding to the vertical geometery, is given by[10] Eq. (2) below, where we have only kept the first two terms. Notice that z_0, and hence z, are temperature dependent.

$$G(z) = \frac{1}{2}\left[1 - \frac{z}{(z^2 + a^2)^{1/2}}\right] - \frac{3b^2a^2z}{16(z^2 + a^2)^{5/2}} + \cdots \qquad (2)$$

where $z = z_0 - x$.

In general, the intensity of radiation reaching the detector from the sample is obtained using Eqs. (1) and (2) and summing over the contributions from all sample slices. Eq.(3) shows the result for the 22-keV K_α x rays where: G(z), expressed as a function of x, is the solid-angle geometrical factor, $\mu_{K\alpha}$ is the

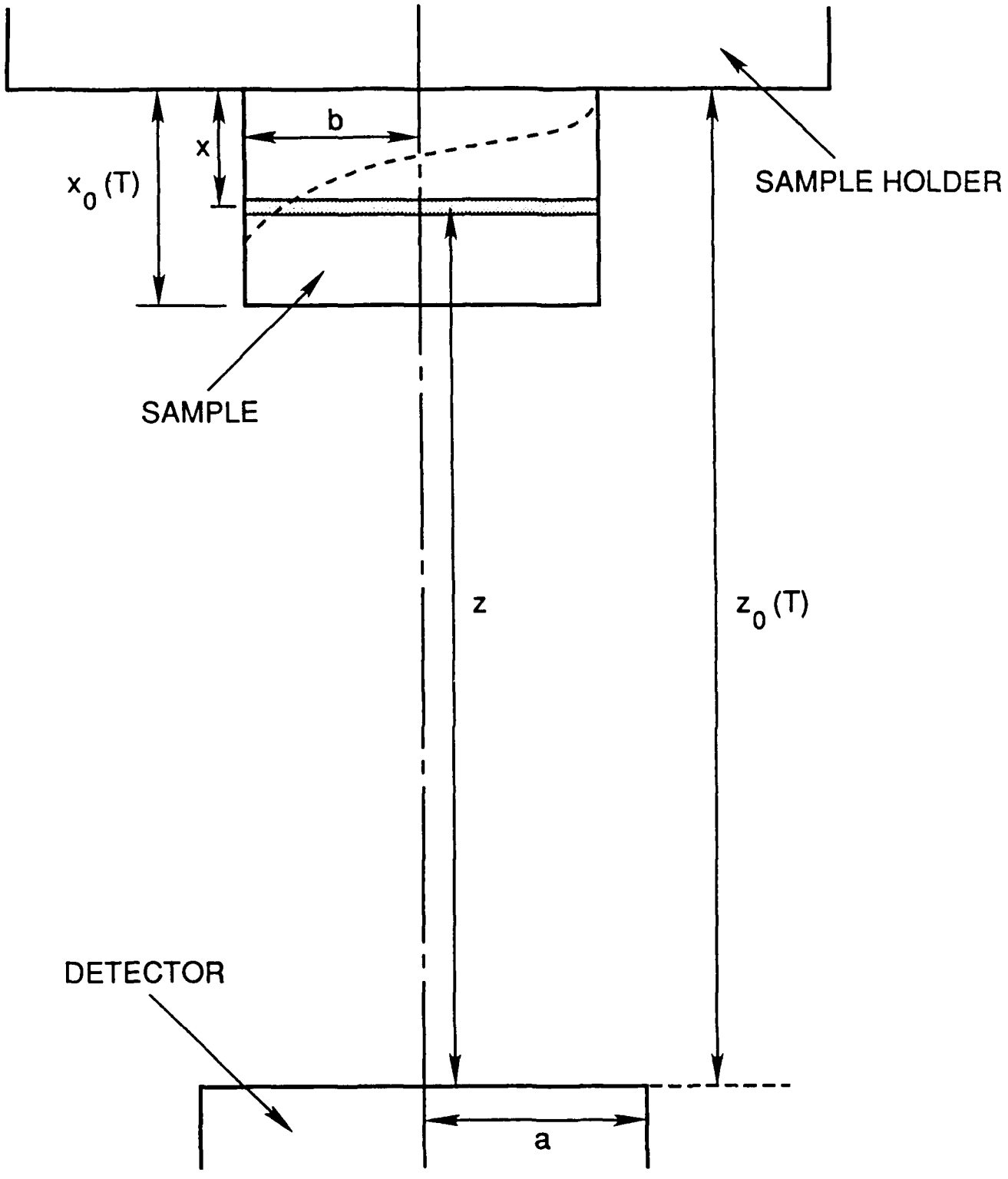

FIG. 1. A schematic represention of the experimental configuration in the vertical geometry. Notice the temperature dependence of z_0 and x_0 due to the contraction of the materials as the temperature is lowered. The solid angle subtended by the detector is thus temperature dependent.

absorption coefficient (mass absorption coefficient times the density), λ is the source decay constant, and x_0 is the sample thickness.

$$I_{K\alpha} = C_{K\alpha} C_0 \lambda e^{-\mu_{K\alpha} x_0 - \lambda t} \int_0^{x_0} G(x) e^{-\alpha x^2 + \mu_{K\alpha} x} dx \qquad (3)$$

where $C_{K\alpha}$ is a constant.

There is a similar expression, Eq. (4), which expresses the result for the 88-keV γ radiation. In this case, there is an additional factor associated with the possible occurrence of nuclear γ-ray resonance absorption i.e. the M.E..

$$I_\gamma = C_\gamma C_0 \lambda e^{-\mu_\gamma x_0 - \lambda t} \int_0^{x_0} G(x) e^{-\alpha x^2 + \mu_\gamma x} dx \left[(1-f) + f e^{-\mu_N x_N} \right] \qquad (4)$$

where: C_γ *is a constant*, μ_γ *is the electronic absorption* coefficient, μ_N is the nuclear-resonant absorption coefficient evaluated on resonance, x_N is the effective-Mössbauer-thickness parameter, and f is the recoilless fraction.

Keep in mind that in Eqs. (3) and (4), C_0, $\mu_{K\alpha}$, μ_γ, μ_N, f, x_0, and G(x) are all temperature dependent. If one considers the ratio of the number of K_α x rays to the number of 88-keV γ rays, Eq. (5), some factors in Eqs. (3) and (4) cancel out.

$$R_{K_\alpha \gamma} = \frac{I_{K\alpha}}{I_\gamma} \qquad (5)$$

B. Experimental procedures and results

Our experimental approach has included recording the number of 22-keV K_α x-ray, and 88-keV γ-ray counts reaching the detector as a function of time at a number of different temperatures. At any given temperature, usually a week of counting time was required to obtain sufficient statistics. Therefore, a standard procedure was adopted to ensure that the experimental conditions for each run at a particular temperature were identical. Each run started at the same time of the day, and lasted 22 hours.

Special care was needed to keep the solid- angle factor the same, since it varies according to the levels of the cryogenic fluids in the helium cryostat. The levels of the cryogenic fluids were initially set at specific values and then maintained in an identical fashion for each run. The data points, at a given temperature, as a function of time should follow the decay curve for ^{109}Cd. Thus, it was possible to examine the value obtained for each run and monitor the performance of the apparatus to determine if there was an undetected problem.

In general these data show a time dependence governed by the decay of the source nuclei ^{109}Cd, and a temperature dependence due to self-absorption of the sample and solid angle changes. These temperature-dependent solid-angle changes resulted from the relative movement of the sample with respect to the detector. The data were analyzed by fitting them to Eq.(3) and Eq. (4) using a nonlinear least-squares routine. The electronic absorption coefficients for the x ray and γ ray in silver, the nuclear-resonant absorption coefficient, the recoilless fraction, and their temperature dependences are known. Since the decay constant for ^{109}Cd is also known, the adjustable parameters are: the source-distribution parameter α, the effective-Mössbauer-thickness parameter x_N, and the solid-angle parameters. There are one solid-angle parameter for each temperature corresponding to the relative sample-detector positioning. The adjustable parameters were varied in order to obtain the best fit for both the x-ray and γ-ray data <u>simultaneously</u> according to Eqs. (3) and (4).

Previous research[8] to observe the M.E. in ^{109}Ag used the same self-absorption approach. However, they recorded only the number of 88-keV γ-ray counts as a function of time at different temperatures. Our analysis shows that geometrical solid-angle effects are very significant. The x-ray data provide the needed geometrical solid-angle information required to successfully analyze the γ-ray data.

1. Experiments in the vertical geometry

In the vertical geometry (see Fig. 1) the ^{109}Cd-doped Ag single crystal is lying flat and a Ge detector is positioned below. We recorded the number of 22-keV K_α x-ray, and 88-keV γ-ray counts reaching the detector as a function of time at three temperatures: 295 K, 78 K, 4.8 K. These data were recorded over a four week period and the results are shown in Fig. 2. The standard procedure, outlined above, was adopted for collecting the data. From these time dependent data we also determined the ratio of x-ray to γ-ray counts at the temperatures given above. From the individual ratio values for each run at a given

temperature, the average value of the ratio at that temperature was determined. The results are shown in Fig. 3.

The time dependent data were analyzed by fitting them simultaneously to Eqs. (3) and (4) using the nonlinear least-squares fitting routine mentioned above. The value obtained for the effective-Mössbauer-thickness parameter x_N is $4.9 \pm 0.6 \times 10^{-4}$ cm. The value for the source-distribution parameter α is 1180 ± 90 cm^{-2}.

In a similar fashion we fit the ratio results (see Fig. 3) to Eq. (5) with the nonlinear least-squares routine outlined above. The values obtained for the effective-Mössbauer-thickness parameter and source-distribution parameter using this ratio method are the same as those determined by fitting the time dependent data using only Eqs. (3) and (4). The precise values obtained by each method corresponding to the best chi-square value were slightly different but the set chosen above fitted all the data quite well and is well inside the experimental errors. In this geometry both methods of analysis, simultaneous fitting of the x-ray and γ-ray counts to Eqs. (3) and (4) or fitting the ratio of the counts according to Eq. (5), are basically the same except for the fact that in the ratio method the solid angle parameters do not play any role in fitting the data. This special property of the ratio method, since the solid-angle parameters essentially cancel out, simplifies the fitting routine significantly. In fact, because of this, the normal procedure is to fit the ratio data first in order to obtain a reasonably good value of the source-distribution parameter α. This value of α is then used as an initial "guess" in fitting the x-ray and γ-ray time dependent data. Because of the rather large number of parameters needed to fit the time dependent data, it is helpful to have reasonably good initial values in order that the least-squares routine converge easily.

2. Experiments in the horizontal geometry

In our experiments in the vertical geometry[1-3], the detected photons fell along the gravitational field. We have also carried out such experiments in the horizontal geometry. In this geometry, the detected photons travel a path roughly perpendicular to the gravitational field. Figure 4 shows the experimental arrangement for this configuration. The details of the experimental procedure are the same as those described above. We have measured the counting rates as a function of time for the x rays and the γ rays at four temperatures: 295 K, 190 K, 78 K, and 4.9 K. The results are shown in Fig. 5. It is important to re-emphasize that the temperature dependence of the solid angle can play a major role in these counting-rate changes. Our data

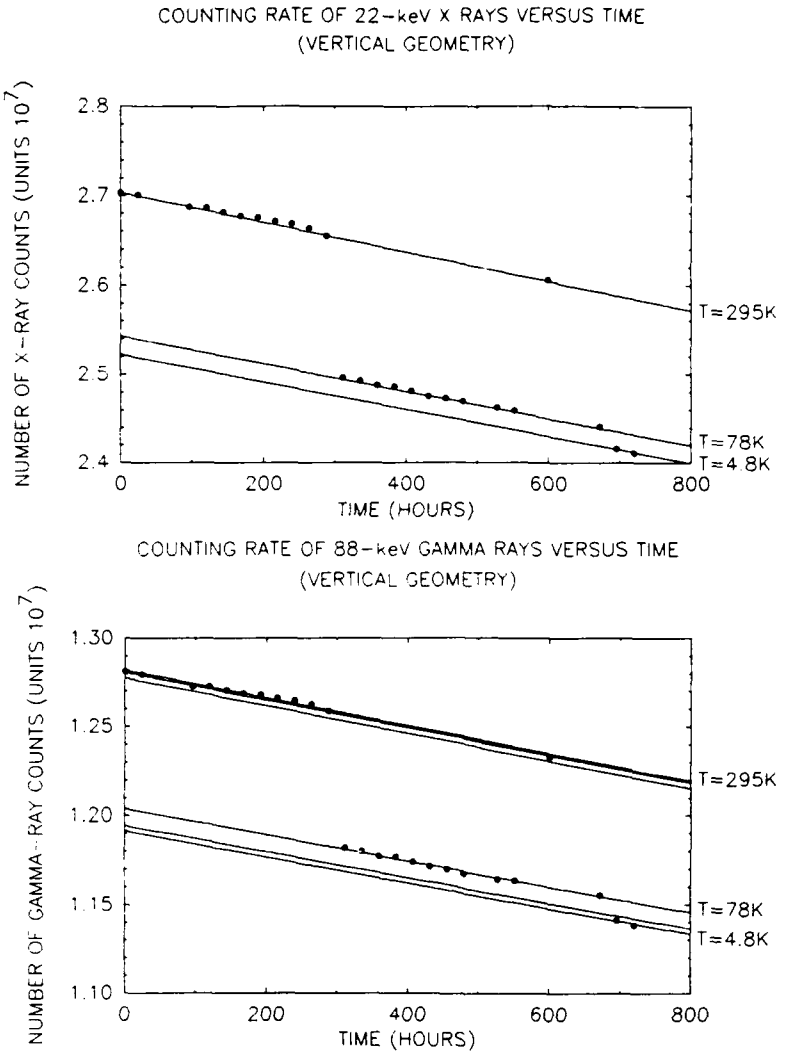

FIG. 2. The top half of the figure shows our experimental data, taken in the vertical geometry, for the counting rate of the 22-keV x rays as a function of time with the sample at three different temperatures. The solid lines are obtained our nonlinear least-squares fitting procedure. The drop in the counting rates as the temperature decreases is due to self absorption and the geometrical solid-angle effects. In the lower half of the figure, similar data for the 88-keV γ rays are recorded. The three parallel lines in upper part of the lower half of this figure correspond to the calculated results at the three temperatures excluding the geometrical solid-angle contribution. The two parallel lines at the bottom show the effect with and without Mössbauer absorption. The values obtained from this procedure for the effective-Mössbauer-thickness parameter x_N is $4.9\pm0.6 \times 10^{-4}$ cm, and for the source distribution parameter α is 1180 ± 90 cm^{-2}.

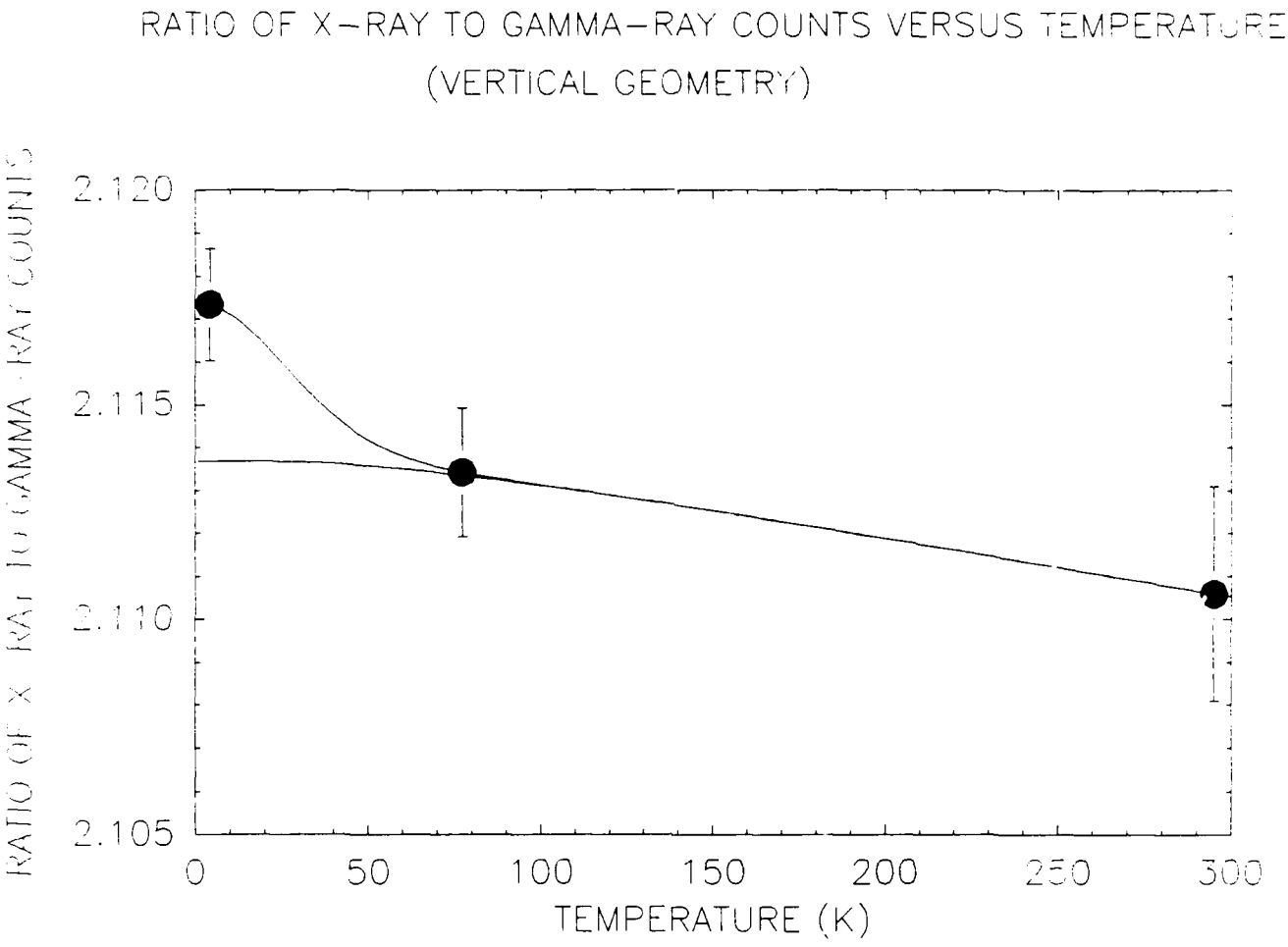

FIG. 3. Our experimental results, using the vertical geometry, for the ratio of 22-keV x-ray to 88-keV γ-ray counts at three temperatures namely 4.8 K, 78 K and 295 K are indicated by the symbols. The two solid curves, obtained by a nonlinear least-squares fitting routine, show our theoretical analysis. The lower one on the left is obtained by putting the Mössbauer effect equal to zero. The higher one includes the presence of the Mössbauer effect. Of course, both curves merge into one at higher temperatures as the Mössbauer effect goes to zero. This analysis yields the following values: the effective-Mössbauer-thickness parameter $x_N = 4.9 \pm 0.6 \times 10^{-4}$ cm and a source distribution parameter $\alpha = 1180 \pm 90$ cm^{-2}.

for the counting rates of the x rays in Fig. 5 clearly show this. As is seen, the counting rates at 4.9 K are higher than the counting rates at 78 K, which is contrary to one's expectations. This behavior is explained by referring to the schematic diagram of the experimental configuration in Fig. 4. Our sample at room temperature was misaligned with respect to the detector and its center was below the center of the detector. As the temperature was lowered, the sample holder and cryostat components contracted. Thus, the sample moved up giving rise to an increase in the solid angle subtended by the detector. The change in the solid angle is largest when the temperature is lowered from 78 K to 4.9 K. This is due to further contractions of the cryostat components. In addition to solid angle changes, the effective path traversed by the photons in the silver sample changes with temperature. As the sample moves up or down relative to the detector this effective path length varies. Therefore, Eqs. (3) and (4) need to be modified.

$$I_{K\alpha} = C_{K\alpha} C_0 \lambda e^{-\mu_{K\alpha}(x_0)_{eff} - \lambda t} \int_0^{x_0} G(x) e^{-\alpha x^2 + \mu_{K\alpha} x_{eff}} dx \qquad (3')$$

and

$$I_\gamma = C_\gamma C_0 \lambda e^{-\mu_\gamma (x_0)_{eff} - \lambda t} \int_0^{x_0} G(x) e^{-\alpha x^2 + \mu_\gamma x_{eff}} dx \left[(1-f) + f e^{-\mu_N (x_N)_{eff}} \right] \qquad (4')$$

where the effective distance $x_{eff} = (x/\cos\phi)$, see Fig. 4.

The data for this geometry were analyzed in a fashion similar to those for the vertical geometry. The x-ray and γ-ray data were simultaneously fitted to Eqs. (3') and (4'), using a non-linear least-squares fitting routine. The adjustable parameters are: the effective-Mössbauer-thickness parameter, the source distribution parameter, and parameters associated with the misalignment of the sample and detector. This misalignment is represented by h in Fig. 4. The value of h changes as the temperature is varied. Therefore, this introduces one additional parameter, misalignment, for each temperature corresponding to the vertical position of the sample relative to the detector. (The change in position in the horizontal direction is quit small due to the contraction of a ¼ inch copper sample mount and is also taken into account.) Finding a solution for this least-

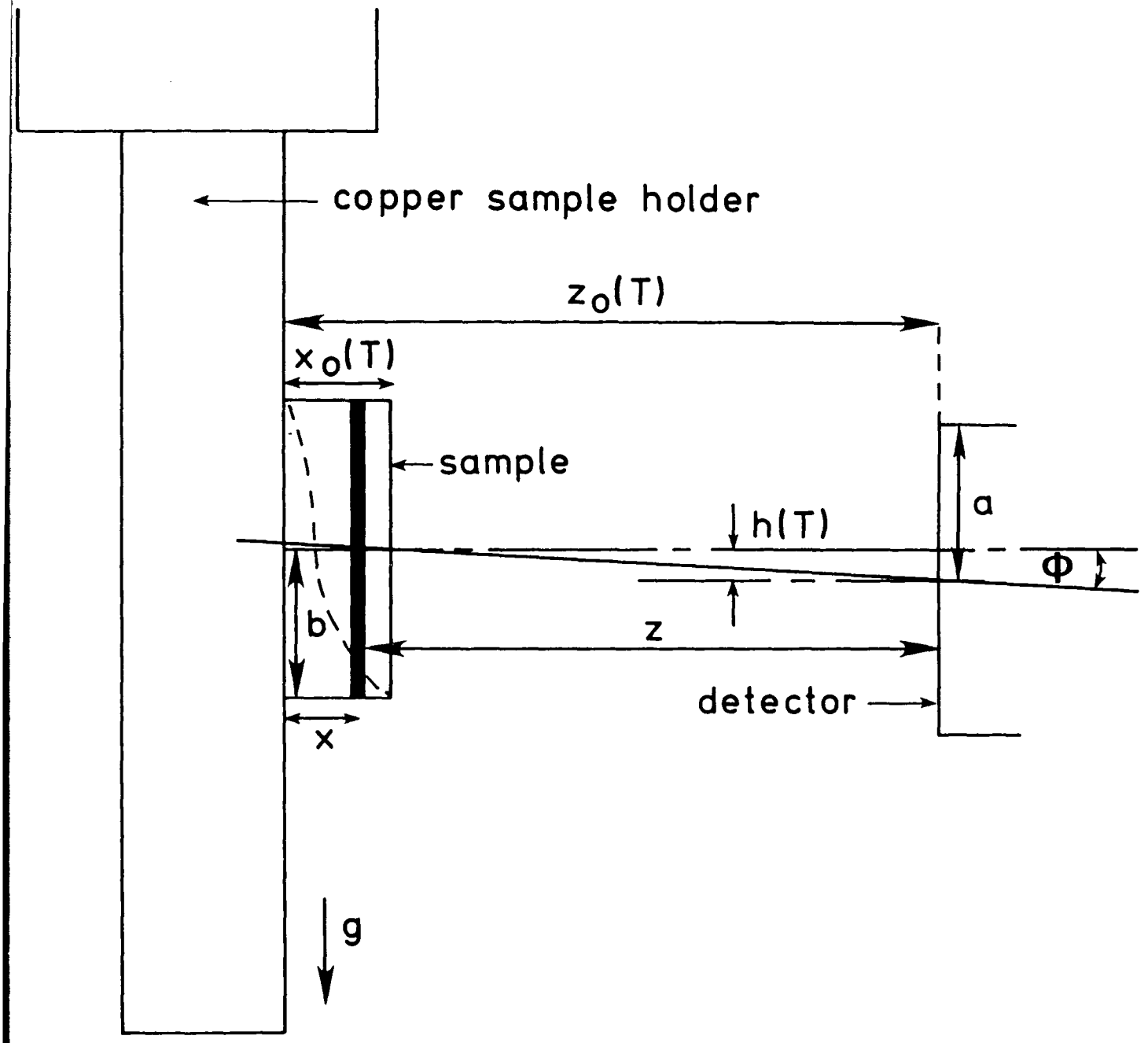

FIG. 4. A schematic representation of the experimental configuration in the horizontal geometry. Notice that the solid angle subtended by the detector is temperature dependent due to the contraction of the materials as the temperature is lowered. Particularly, note that the sample moves up as the temperature is lowered. The values of the parameters are as follows: $x_0(295) = 5.21 \times 10^{-2}$ cm, $z_0(295) = 6.45$ cm, $a = 0.50$ cm, and $b = 0.48$ cm. The misalignment parameter is h(T).

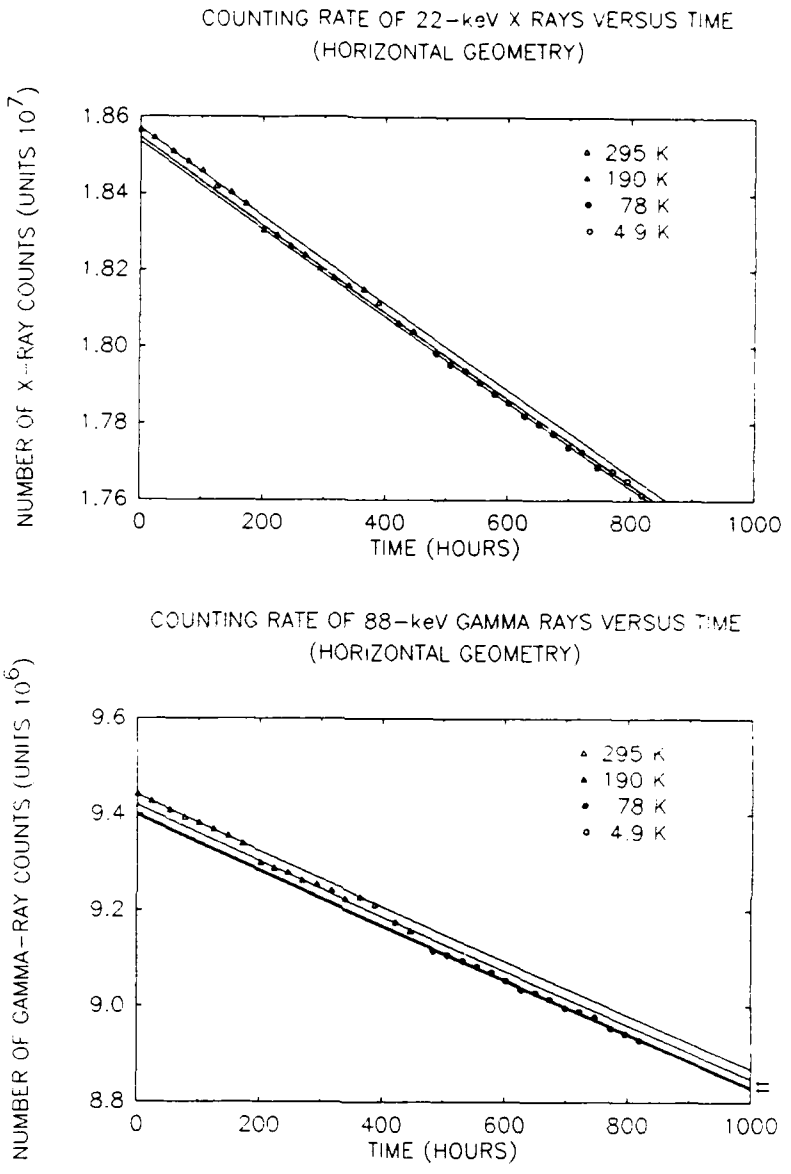

FIG. 5. The top half of the figure shows the data, taken in the horizontal geometry, for the 22-keV x rays as a function of time at four temperatures. Notice that the counting rate at 4.9 K is higher than expected. The lower half of the figure shows our experimental data for the counting rate of the 88-keV γ rays. The solid lines are obtained by a nonlinear least-squares fitting procedure described in the text. The two arrows on the side of the figure focus attention on the three solid lines corresponding to the three cases: 78 K, 4.9 K including the M.E., and 4.9 K excluding the M.E.. Notice that the size of the M.E. is almost undetectable.

squares problem is a very difficult task due to the large number of adjustable parameters relative to the number of data points. However, since the vertical thermal contractions of the sample mount and the cryostat components in this geometry are the same as those in the vertical geometry one can use the fitted solid-angle parameters in the vertical geometry to reduce the number of the misalignment parameters in the horizontal case. Thus, the misalignment parameters can be represented by $h_0+\Delta h$, where h_0 is a constant that represents the initial, i.e., room temperature, vertical misalignment of the sample and detector, and Δh is a temperature dependent parameter that can be obtained from the analysis of the data in the vertical geometry. This allowed the least-squares fitting routine to function effectively and yield a value for the effective-Mössbauer-thickness parameter x_N of $4\pm2 \times 10^{-5}$ cm and a value for the source-distribution parameter α of 1400 ± 100 cm^{-2}. Notice that in this case the size of the M.E. is at least an order of magnitude smaller than in the vertical geometry. The value obtained here for the source-distribution parameter is different from the one determined in the vertical geometry because of the fact that the vertical experiment was carried out first and then the sample was cleaned before performing the horizontal experiment. In the cleaning process some of the radioactivity was removed from the sample.

In this geometry the ratio of the x-ray to the γ-ray counts, contrary to the case in the vertical geometry, could not be anaylzed independently due to the addition of the misalignment parameters. When the ratio of the counts is calculated using Eqs. (3′) and (4′), the number of adjustable parameters is not sufficiently reduced to allow an independent fitting. However, for the sake of comparison with the ratio results in the vertical geometry, we used the values of the fitted parameters from the simultaneous fitting of the x-ray and γ-ray data to Eqs. (3′) and (4′) to simulate the ratio results. Figure 6 shows these results.

C. Formulation of the problem from a more fundamental approach: connection with the parametric formulation

In this experimental technique the intensity of the γ radiation in a particular direction is measured. The intensity of the γ radiation reaching the detector from the sample is given by Eq. (4). The time dependence can be accounted for and many of the above factors are unimportant for the present discussion. In fact, only the last term in Eq. (4) is needed.

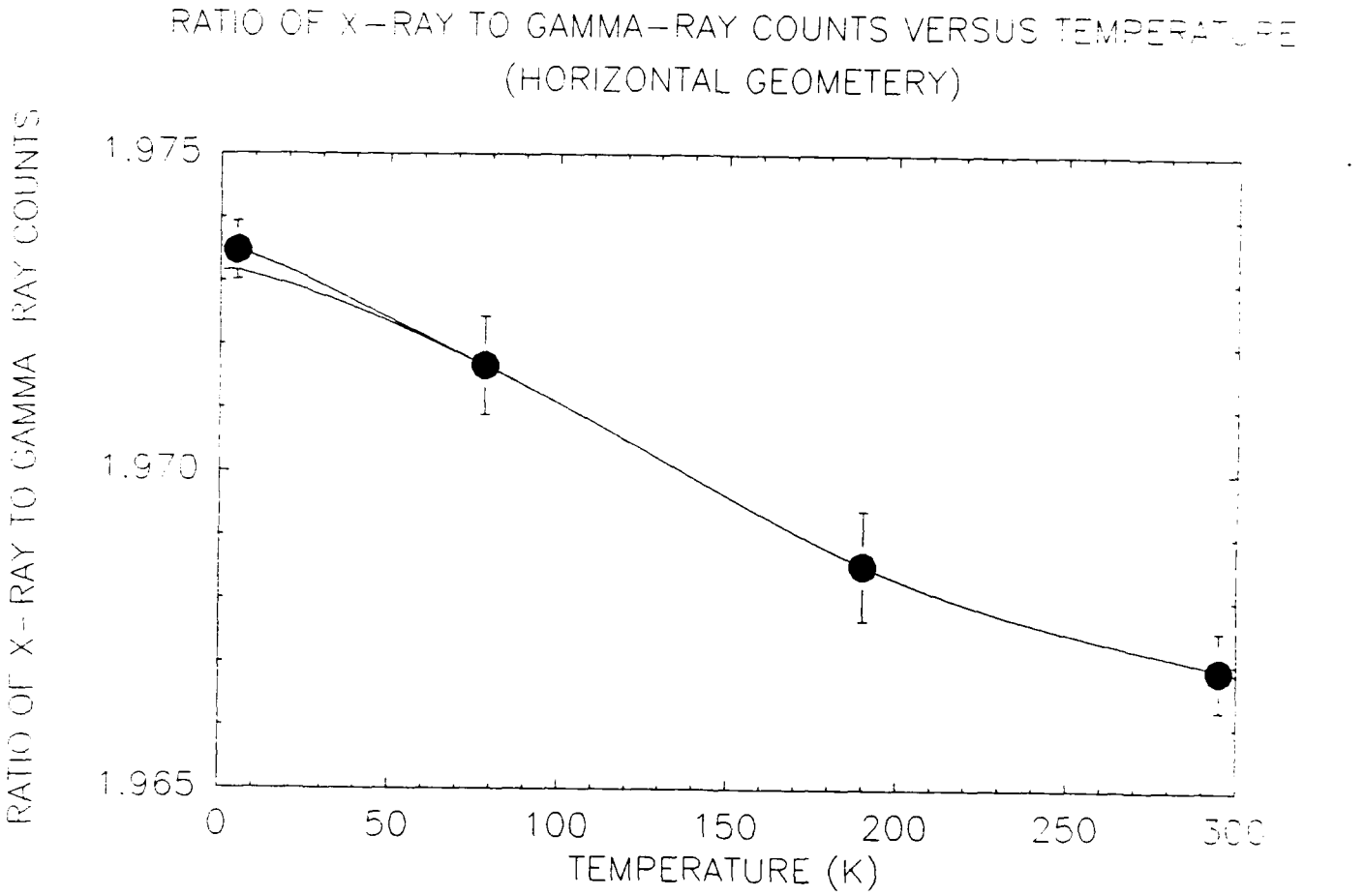

FIG. 6. The experimental results in the horizontal geometry for the ratio of 22-keV x-ray to 88-keV γ-ray counts at four temperatures; namely 295 K, 190 K, 78 K, and 4.9 K for the horizontal geometry. The two solid curves show the simulated results using the values of the parameters determined from an analysis of the time-dependent data. The lower curve is obtained by putting the Mössbauer effect equal to zero. The higher one includes the presence of the Mössbauer effect. Notice that the size of the M.E. for this case is vanishingly small considering the indicated experimental error.

$$I'_\gamma = \int_0^{x_0} G(x) e^{-\alpha x^2 - \mu_\gamma x} f e^{-\mu_N x_N} dx \qquad (6)$$

In this equation, as in Eq. (4), μ_N is the value of the nuclear- resonant absorption coefficient <u>on</u> resonance and x_N is the effective-Mössbauer-thickness parameter indicating the size of the M.E.. In order to proceed further one must relate x_N to the physical parameters that occur in a more complete theoretical treatment of the problem. In the experiment, the detector records all photons over an energy range that is large compared to the emission or absorption nuclear-resonant line shape even in the presence of a large magnetic field. Therefore, a more complete and explicit reformulation of Eq. (6) can be written as,

$$I'_\gamma = f \int dE\ S(E) \int_0^{x_0} dx G(x) e^{-\alpha x^2 - \mu_\gamma (x_0 - x)} e^{-A(E)(x_0 - x)} \qquad (7)$$

where S(E) is the nuclear-resonant emission line shape and A(E) is the energy-dependent nuclear-resonant absorption coefficient.

Using the parametric form of the intensity transmitted, Eq. (6), together with the more fundamental approach, Eq.(7), one can obtain the value of the effective-Mössbauer-thickness parameter x_N in terms of more realistic physical parameters,

$$x_N = \frac{1}{A(E_0)} \ln \left[\frac{\left[\int_0^{x_0} G(x) e^{-\alpha x^2 - \mu_\gamma (x_0 - x)} dx \right] \left[\int dE\ S(E) \right]}{\int dE\ S(E) \int_0^{x_0} dx\ G(x) e^{-\alpha x^2 - \mu_\gamma (x_0 - x)} e^{-A(E)(x_0 - x)}} \right] \qquad (8)$$

where, since E_0 is the resonance energy, $A(E_0) = \mu_N$ is the nuclear-resonant absorption coefficient evaluated <u>on</u> resonance.

In order to obtain a clearer picture of the significance of the parameters, we will now present some explicit calculated results for ^{109}Ag in silver. (See the APPENDIX for a summary of values used in these calculations.) First, consider the case when the emission line shape and absorption cross section are of the single-line Lorentzian shape. It is not difficult to incorporate in the calculations a shift of the absorption cross section relative to the emission line shape, as well as an increase in the absorption linewidth. Under these circumstances one can calculate the value of the effective-Mössbauer-thickness parameter x_N, which is a measure of the size of the M.E., versus the various other parameters according to Eq. (8).

Figure 7 shows the results for x_N versus the source distribution parameter α. Increasing α corresponds to the case in which the radioactivity is more localized on one side of the sample. The transmission of the γ rays is recorded when viewing the sample from the other side. Thus, if the M.E. is occurring, the effective-Mössbauer-thickness parameter x_N should increase as α increases. This is shown in the figure and indicates an increasing M.E. as α increases.

Similarly, the effect of broadening the absorption cross section for this "single-line" case can be deduced. Figure 8 shows some results under these conditions using a fixed value of α. As one expects, the size of the M.E. (characterized by x_N) decreases as the nuclear-resonant absorption cross section effective linewidth increases. Figure 9 shows calculated results using a particular source distribution parameter α and the natural linewidth for both the emission line shape and absorption cross section, but now a shift is introduced so that the maxima in the emission line shape and absorption cross section do not coincide in energy. As expected, the size of the M.E. decreases as the relative shift of the absorption cross section increases.

Of course calculations of this sort can be made using more complicated line shapes by, for example, including a magnetic field. Using this approach, model calculations can be made. The presence of inhomogeneous fields can be approximated by introducing a broadened nuclear-resonant cross section and a relative shift with respect to the emission line shape. Calculations including the presence of an applied magnetic field are given in the next section.

D. A new experimental technique for detecting recoilless γ-ray transitions in long-lived nuclear levels.

Discovering and developing techniques for obtaining better energy resolution has been a continuing scientific endeavor. A pertinent example is the discovery of recoilless nuclear-resonant

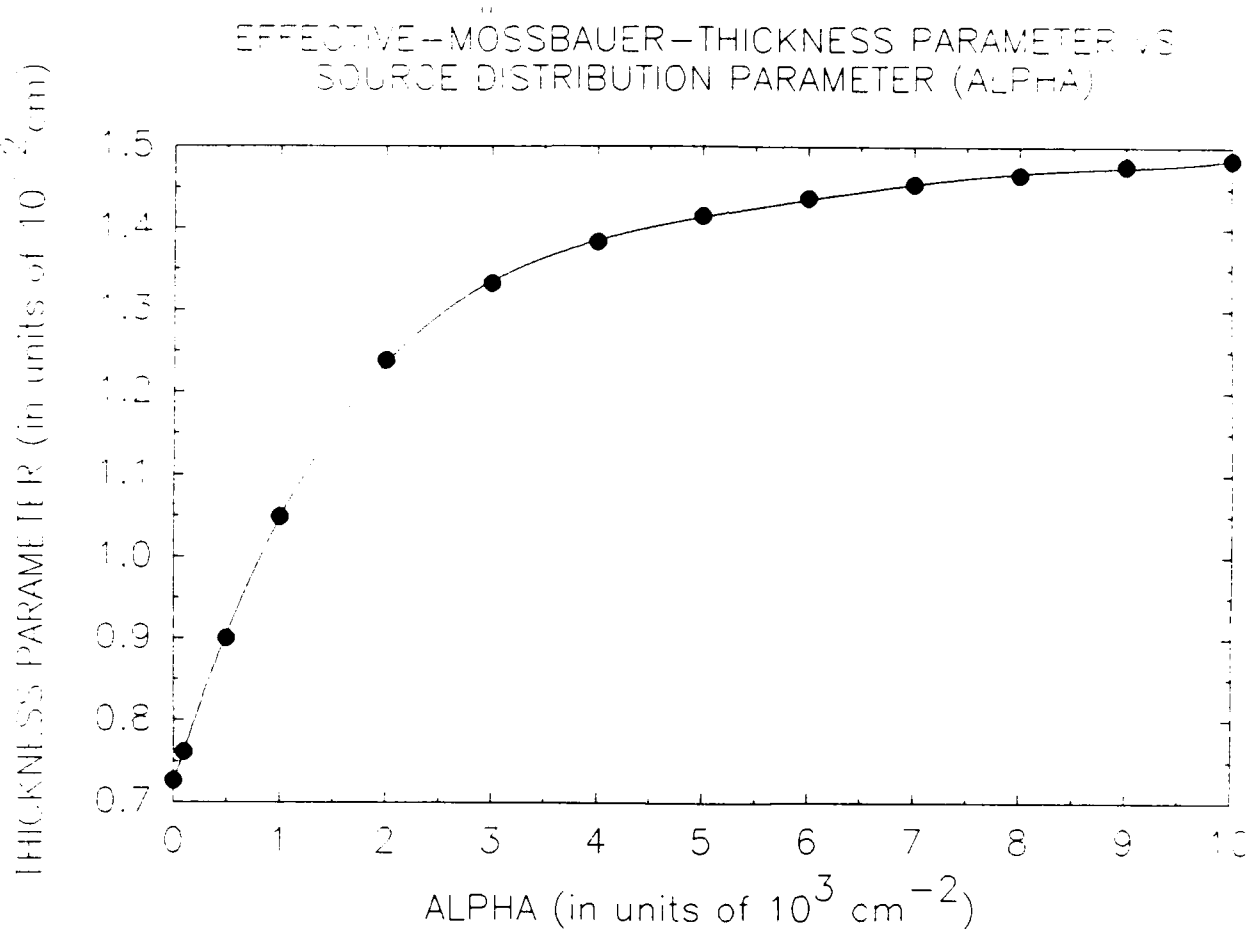

FIG. 7. Using the 88-keV 40-sec transition in ^{109}Ag and the other conditions described in the APPENDIX, the effective-Mössbauer-thickness parameter is calculated versus the source distribution parameter α. The emission line shape and absorption cross section coincide in energy and are assumed to be of the single-line Lorentzian type with natural linewidth. (The calculated values are shown as solid circles, while the solid line is simply an aid to the eye.)

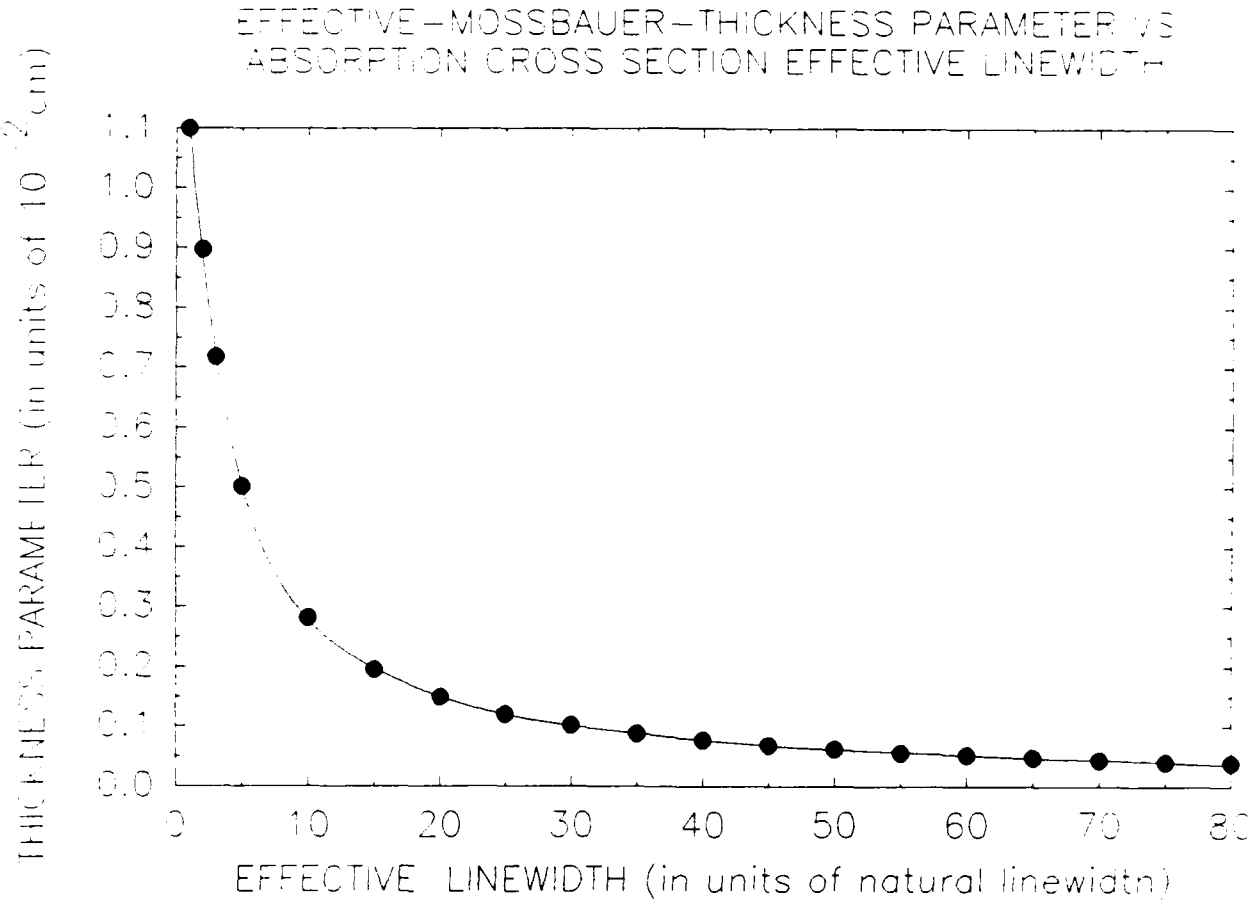

FIG. 8. Calculated results for the ^{109}Ag effective-Mössbauer-thickness parameter are shown as a function of the absorption cross section effective linewidth assuming the additional parameters as described in the APPENDIX. The emission line shape is assumed to be of the single-line Lorentzian type with natural linewidth. The maxima in the emission line shape and absorption cross section coincide in energy. The source distribution parameter α is held fixed. (The calculated values are shown as solid circles, while the solid line is simply an aid to the eye.)

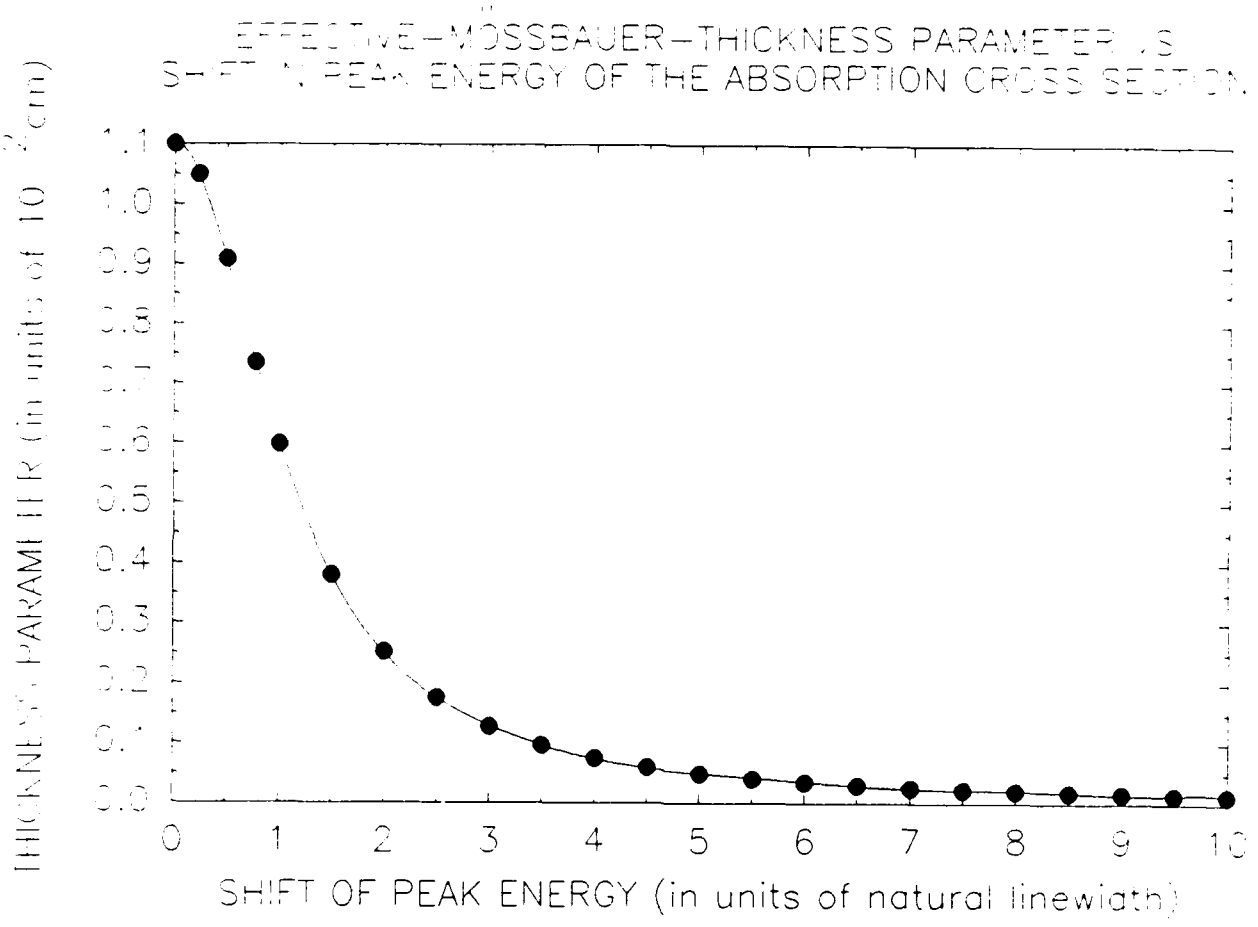

FIG. 9. Calculated results for the ^{109}Ag effective-Mössbauer-thickness parameter are shown as a function of the shift in the peak energy of the absorption cross section assuming the additional parameters as described in the APPENDIX. The emission line shape and absorption cross section are assumed to be of the single-line Lorentzian type with natural linewidth. The source distribution parameter α is held fixed. (The calculated values are shown as solid circles, while the solid line is simply an aid to the eye.)

radiation, i.e., the M.E.[11], which allowed the direct observation of hyperfine structure. Additionally, this discovery was used to study the gravitational red shift[12-14]. In utilizing the M.E. a question arises as to the observation of such an effect using nuclear states having progressively longer lifetimes and correspondingly narrower linewidths. Under ultra-narrow conditions, i.e., lifetimes on the order of seconds, it becomes clear that the method used in conventional Mössbauer spectroscopy of doppler shifting a source with respect to an absorber is untenable due to unavoidable and uncontrollable relative motion caused by electrical and mechanical vibrations at this level of precision. In spite of the difficulties, the existence of ultra-narrow nuclear-resonant states would have considerable impact on: the possible development of γ-ray lasers, the determination of the size and extent of inhomogeneous fields in solids, and the continuing study of the gravitational red shift.

The search for ultra-narrow nuclear-resonant states has, as noted above, often utilized the self-absorption technique. In this technique, recoilless nuclear-resonant absorption (i.e. the M.E.) is detected by observing the increased absorption of a sample at low temperatures. In this procedure there are a number of experimental parameters, as described above, that change as the temperature is lowered that are <u>not</u> due to the occurrence of the M.E. thus making positive identification difficult. Here we describe a self-absorption technique in which the sample is held at a <u>fixed</u> low temperature and a magnetic field is applied in different orientations.

The purpose of this section is to investigate procedures for observing ultra-narrow nuclear-resonant states using a modified version of the self-absorption technique . The basic idea utilizes a sample which contains both source and absorber nuclei. As the temperature of the sample is lowered the "recoilless fraction" increases, and the radiation coming out of the sample decreases indicating nuclear-resonant absorption. Experiments such as these are described above. Difficulties arise in such experiments primarily due to the fact that as the temperature is lowered there will be changes in the counting rates as the solid angle subtended by the detector changes. This is caused by contraction of various parts of the apparatus and sample mount as the temperature decreases. Indeed, the density of the sample itself changes with temperature and the counting rates are further affected. Unless extreme care is taken, or appropriate corrections are made, very misleading conclusions can be drawn from such experiments.

In this section we explore the consequences of this self-absorption technique when incorporating an externally applied

magnetic field. It will be shown that it may be possible to confirm the occurrence of the M.E. when the sample is held at a constant low temperature while, in addition, subjected to a externally applied magnetic field of different orientations. In order to get a feeling for where this development is leading, consider Eq. (7) ignoring all the factors due to different sample slices and the electronic absorption, and treating the nuclear-resonant part in the "thin" absorber limit.

$$I'_{\gamma} \propto \int dE\, S(E)\left[1 - A(E)\right] \qquad (9)$$

The important factor is the product of the emission line shape and absorption cross section summed over energy. The largest value for the absorption will occur for the case in which S(E) and A(E) are of "single-line" line shape and the maxima of each coincide in energy. If S(E) and A(E) are split in several lines, corresponding to the case of the sample's nuclei being subjected to an externally applied magnetic field, the absorption will decrease. In this case the absorption will be maximum when the spectrum is split into the fewest number of lines. Since the selection rules govern this result, the absorption will depend on the angle between the gamma-ray observation direction and the direction and size of the applied magnetic field. It is perhaps worth pointing out that if the experiment were of the usual M.E. type, where the emission line shape is doppler shifted over the absorption cross section, the result would be <u>independent</u> of the line shape.

Because of our interest in observing the M.E. in ^{109}Ag, we have made calculations for this case. However, the general principles will apply in a similar fashion to any other case. As noted above, the single-line case would produce the largest M.E using the self-absorption technique. Assuming a line shape consisting of a single line for these ultra-narrow Mössbauer transitions is unrealistic in that, at the very least, the sample is subjected to the earth's magnetic field. Moreover, to produce the zero magnetic field condition with the precision required by ultra-narrow states ($\approx 10^{-6}$ gauss) may be unfeasible.

In this section results will be presented using the ^{109}Ag case (see the Appendix for a summary of values used in the calculations) while subjecting the sample to an externally applied magnetic field. In Fig. 10 results are plotted to show the effect of increasing the strength of the applied magnetic field. At zero magnetic field the nuclear-resonant absorption is a maximum, corresponding to the "single-line" case above. As the magnetic field strength increases, the emission and absorption

line shapes split into components governed by the selection rules. Once the line shape has split into its separate components, further increase in the magnetic field strength has little effect on the nuclear-resonant absorption. The line shapes corresponding to three different orientations (theta) of the applied magnetic field relative to the γ-ray observation direction are given in Fig. 11. As should be clear from the above discussion and the results shown in Fig. 11, the M.E. as a function of angle of the applied magnetic field should be largest at theta = 0°, smallest at theta = 45°, and intermediate at theta = 90°. Figure 12 shows the results of calculations for various values of theta.

None of the experiments, searching for the M.E. in ^{109}Ag, have obtained results which correspond to the observation of the natural linewidth (1.15×10^{-17} eV). This is not surprising. Therefore, in order to make an evaluation of the potential of the technique described here, one should calculate results for both the ideal and more realistic cases. The ideal case is obtained by assuming that the emission and absorption line shapes coincide in energy and are composed of lines having the natural linewidth. Considering the particular case of ^{109}Ag in a silver single crystal these specific calculations indicate, that by changing the orientation of the applied magnetic field of 0.5 gauss with respect to the observation direction from 0° to 45°, the change in the γ-ray counting rate is 0.7%. (The largest value of x_N for this ideal case is 1.1×10^{-2} cm.)

However, our latest value for the effective-Mössbauer-thickness parameter x_N does not correspond to the ideal case, but is in fact equal to about 5.0×10^{-4} cm. In order to make a more realistic evaluation, we assumed an applied magnetic field of about 0.5 gauss oriented at 45° with respect to our observation direction. These conditions corresponded roughly to our experimental situation. For this case we determined the broadening of the absorption cross section required to produce the observed value of x_N. Using this broadened cross section we calculated the case when theta equals 0°. The change in the counting rate for this more realistic case amounted to approximately 0.3%.

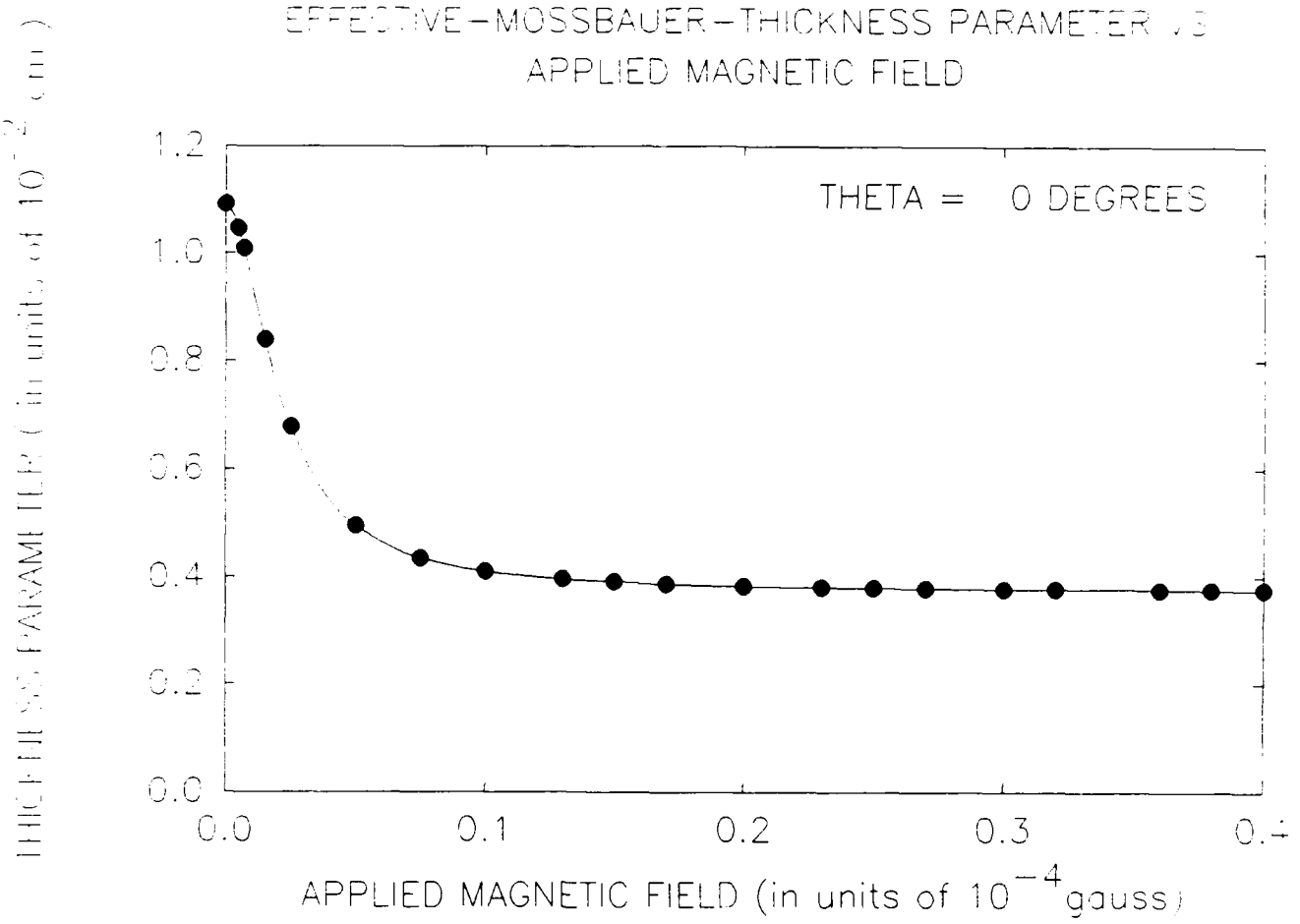

FIG. 10. The effective-Mössbauer-thickness parameter is calculated versus the strength of an applied magnetic field. The emission and absorption line shapes are assumed to coincide in energy and to consist of lines having natural linewidth. The direction of the applied magnetic field is in the same direction as the observation direction for the γ-ray emission, i.e., theta = 0°. The source distribution parameter α is held fixed. (The calculated values are shown as solid circles, while the solid line is simply an aid to the eye.)

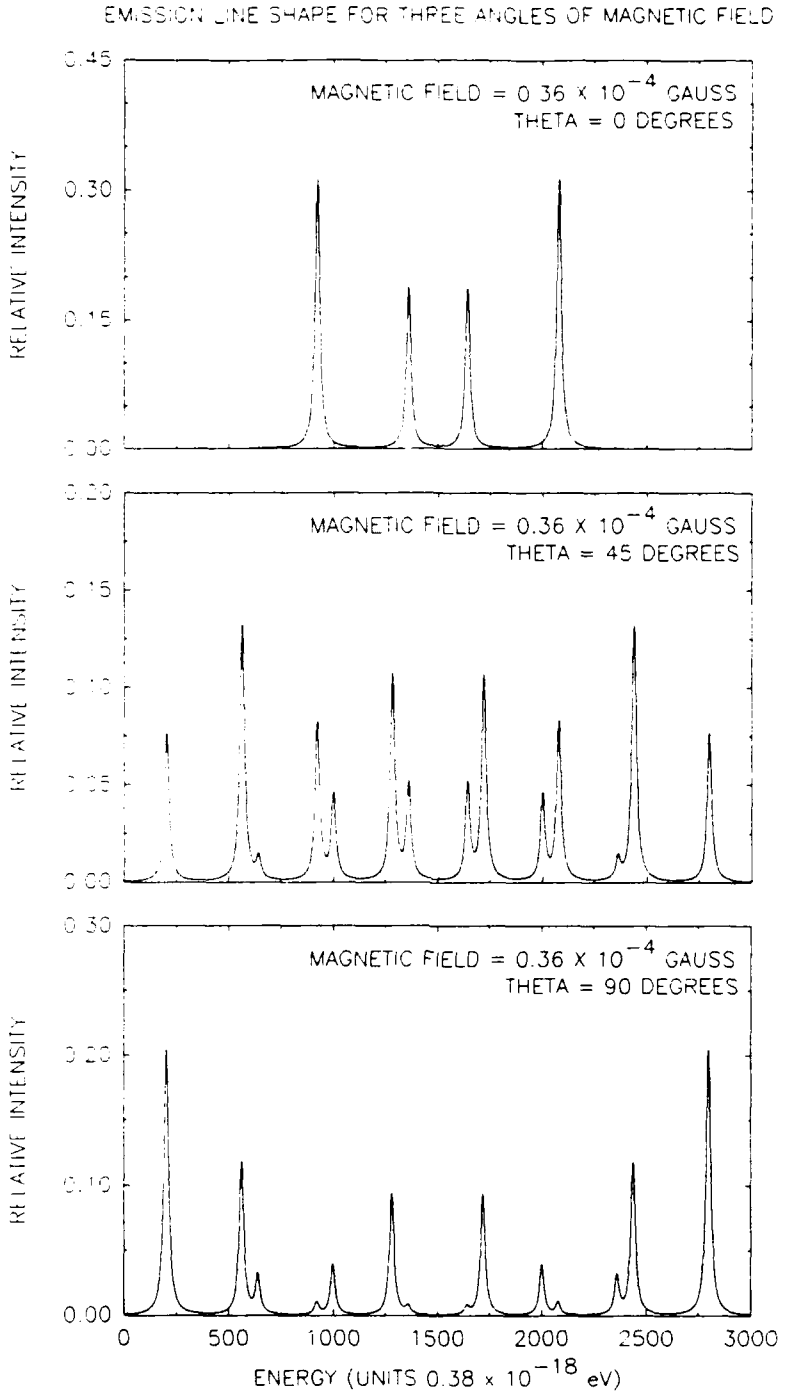

FIG. 11. The emission line shape, assuming lines of natural linewidth, is shown for three angles of the applied magnetic field relative to the observation direction. The magnetic field is held fixed at 0.36×10^{-4} gauss.

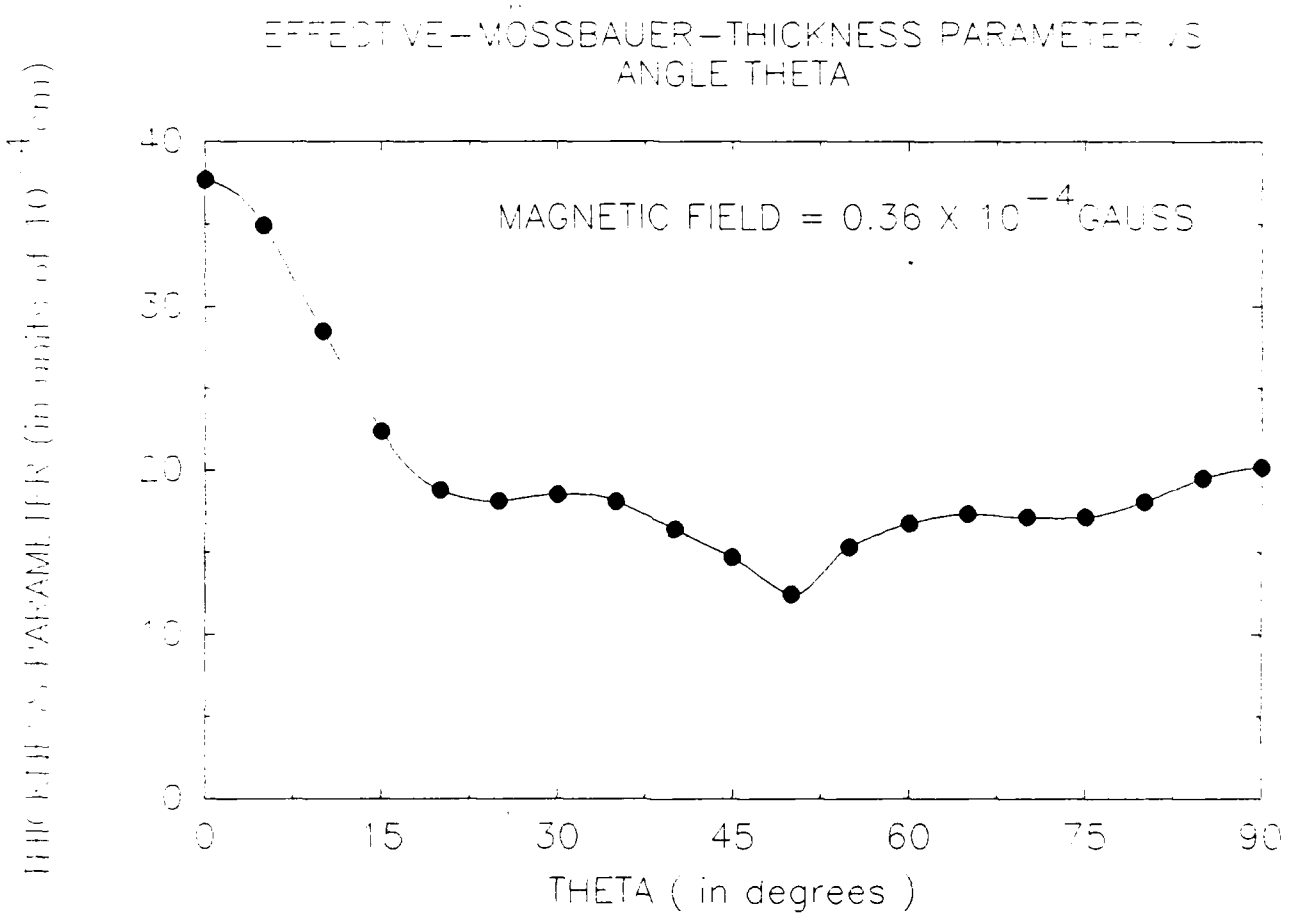

FIG. 12. Calculations are shown for the value of the effective-Mössbauer-thickness parameter versus the angle between the observation direction and direction of the applied magnetic field. The emission and absorption line shapes are assumed to coincide in energy and to consist of lines having natural linewidth. The magnetic field is held constant at 0.36×10^{-4} gauss. The source distribution parameter α is held fixed. (The calculated values are shown as solid circles, while the solid line is simply an aid to the eye.)

V. CONCLUSIONS

Our results indicate that the M.E. is occuring for the 88-keV transition of ^{109}Ag in silver single crystals. Furthermore, the effect appears to be an order of magnitude smaller in the horizontal geometry than in the vertical geometry. Using our model calculations, the size of the M.E. in the vertical geometry is consistent with a line broadening factor of only about 5. This would appear to be an unphysical result. These results suggest that gravitational sweeping is playing a significant role in producing an observable M.E.. Very soon we will make further model calculations incorporating the gravitational sweeping mechanism in order to evaluate its significance. In addition, we are presently performing further experiments using a thicker silver single-crystal sample which should shed light on this question.

The search for the M.E. in ultra-narrow γ-ray transitions (lifetimes on the order of seconds) is difficult. One of the methods used is based on the increased self-absorption of γ rays emitted in a particular direction as the temperature of the sample is lowered. This increase in absorption at low temperature is an indication of the occurrence of the M.E.. There are substantial difficulties, outlined above, associated with this technique because changes in the γ-ray counting rates as a function of temperature are associated with a number of experimental factors other than the occurrence of the M.E.. In order to substantiate the observation of the M.E., all these other factors must be taken into account as we have demonstrated above.

We have investigated an experimental method that is an extension of the basic self-absorption technique in which an external magnetic field is applied to the sample while the sample is held at a fixed low temperature obviating some of the experimental problems. Considering the particular case of ^{109}Ag in a silver single crystal, these calculations indicate that by changing the orientation of the magnetic field with respect to the observation direction from 0° to 45° the change in the γ-ray counting rate in the ideal case is 0.7%. The estimate for this change assuming more realistic values is 0.3%. Consequently, it may be possible to observe the Mössbauer effect in ultra-narrow nuclear-resonant states using this proposed technique.

APPENDIX: NUMERICAL VALUES USED IN THE CALCULATIONS

The calculated results presented in the main body of this report were done assuming the case of ^{109}Ag. The sample is a ^{109}Cd-doped silver single crystal. ^{109}Cd electron captures with a half-life of 463 days[15] to the first excited state of ^{109}Ag. This state has a spin of 7/2, positive parity, a half-life of 39.6 sec, and a magnetic moment of 4.27 nuclear magnetons. The ground state has a spin 1/2, negative parity, and a magnetic moment of -0.131 nuclear magnetons. The transition is E3 with an energy of 88.03 keV, an internal conversion coefficient of 26.7, and a natural linewidth of 1.15×10^{-17} eV. The recoilless fraction (f) for silver is 5.2% and the number density of silver atoms (n_0) is 5.93×10^{22} cm^{-3} at 4.2 K. The isotopic abundance of ^{109}Ag (P) is 48.7%. The nuclear-resonant cross section on resonance [$\sigma(E_0)$] is 4.57×10^{-20} cm^2 and the atomic absorption coefficient (μ_a) is 21.46 cm^{-1}. The nuclear-resonant absorption coefficient A(E) is equal to $fn_0P\sigma(E)$. The thickness of the silver sample is taken to be 0.05 cm and the source distribution parameter α is assumed to be 1200 cm^{-2} for those cases in which this parameter is held fixed.

REFERENCES

1. G.R. Hoy and R.D. Taylor, J. Quant. Spect. and Rad. Trans., 40, 763 (1988).

2. R.D. Taylor and G.R. Hoy, SPIE Short and Ultrashort Wavelength Lasers 875, 126 (1988)

3. G.R. Hoy, S. Rezaie-Serej, and R.D. Taylor, Proc. Int. Conf. on Applications of Mössbauer Effect, Budapest, Hungary (1989), paper 15.7.

4. S. Rezaie-Serej, G.R. Hoy, and R.D. Taylor, SOQUE Proceedings, LASERS' 89, New Orleans, Louisiana, December 3-8, 1989.

5. R. Coussement, G. Scheveneels, F. Hardeman, and P. Boolchand, Hyperfine Interactions 42, 1169 (1988).

6. G.E. Bizina, A.G. Beda, N.A. Burgov, and A.V. Davydov, Soviet Phys. JETP 18, 973 (1964)

7. V.G. Apatov, A.G. Beda, G.E. Bizina, A.V. Davydov, and M.M. Korotokov, Proc. Int. Conf. on Mössbauer Spectroscopy, Bucharest, Romania (1977).

8. W. Wildner and U. Gonser, J. Phys. (Paris) 40, C2-47 (1979).

9. J. Askill, in Tracer Diffusion Data for Metals, Alloys, and Simple Oxides, (Plenum Pub. Co., New York) 1970.

10. A. H. Jaffey, Rev. Sci. Instrum. 25, 349 (1954).

11. R.L. Mössbauer, Z. Phys. 151, 124 (1958); Naturwissenschaften 45, 538 (1958); Z. Naturforsch. 14a, 211 (1959).

12. R.V. Pound and G.A. Rebka Jr., Phys. Rev. Lett. 3, 439 (1959).

13. R.V. Pound and G.A. Rebka Jr., Phys. Rev. Lett. 4, 337 (1960).

14. R.V. Pound and J.L. Snider, Phys. Rev. Lett. 13, 539 (1964); Phys. Rev. 140, B788 (1965).

15. J. Blachot, Nucl. Data Sheets 41, 111 (1984).